


Intranodal pressure of a metastatic lymph node reflects the response to lymphatic drug delivery system

Shigeki Kato^{1,2,3} | Kazu Takeda^{1,2} | Ariunbuyan Sukhbaatar^{1,2} | Maya Sakamoto^{1,2,4} | Shiro Mori^{1,2,5} | Kiyoto Shiga⁶ | Tetsuya Kodama^{1,2,7} 

¹Laboratory of Biomedical Engineering for Cancer, Graduate School of Biomedical Engineering, Tohoku University, 4-1, Sendai, Aoba, Miyagi 9808575, Japan

²Biomedical Engineering Cancer Research Center, Graduate School of Biomedical Engineering, Tohoku University, Sendai, Japan

³Department of Immunology, Kindai University Faculty of Medicine, Osaka-Sayama, Japan

⁴Department of Oral Diagnosis, Tohoku University Hospital, Sendai, Japan

⁵Department of Oral and Maxillofacial Surgery, Tohoku University Hospital, Sendai, Japan

⁶Department of Head and Neck Surgery, Iwate Medical University, Yahaba-cho, Japan

⁷Department of Electronic Engineering, Graduate School of Engineering, Tohoku University, Sendai, Japan

Correspondence

Tetsuya Kodama, Laboratory of Biomedical Engineering for Cancer, Graduate School of Biomedical Engineering, Tohoku University, 4-1 Seiryō, Aoba, Sendai, Miyagi 980-8575, Japan.

Email: kodama@tohoku.ac.jp

Funding information

Japan Society for the Promotion of Science KAKENHI, Grant/Award Numbers 17K13039, 19K16622, 19K22692, 17K20077, 17H00865, 19K22941, 20H00655.

Abstract

Cancer metastasis to lymph nodes (LNs) almost certainly contributes to distant metastasis. Elevation of LN internal pressure (intranodal pressure, INP) during tumor proliferation is associated with a poor prognosis for patients. We have previously reported that a lymphatic drug delivery system (LDDS) allows the direct delivery of anticancer drugs into the lymphatic system and is a promising treatment strategy for early-stage LN metastasis. However, methods for evaluating the treatment effects have not been established. Here, we used a mouse model of MXH10/Mo-*lpr/lpr*, which develops a systemic swelling of LNs, and murine malignant fibrous histiocytoma-like (KM-Luc/GFP) cells or murine breast cancer (FM3A-Luc) cells inoculated into the subiliac LN of mice to produce a tumor-bearing LN model. The changes in INP during intranodal tumor progression and after treatment with cis-dichlorodiammineplatinum(II) (CDDP) using an LDDS were measured. We found that tumor progression was associated with an increase in INP that occurred independently of LN volume changes. The elevation in INP was suppressed by CDDP treatment with the LDDS when intranodal tumor progression was significantly inhibited. These findings indicate that INP is a useful parameter for monitoring the therapeutic effect in patients with LN metastasis who have been given drugs using an LDDS, which will serve to manage cancer metastasis treatment and contribute to an improved quality of life for cancer patients.

KEYWORDS

breast cancer, cancer treatment, drug delivery, intranodal pressure, lymph node metastasis

Shigeki Kato and Kazu Takeda contributed equally to the research.

This is an open access article under the terms of the Creative Commons Attribution-NonCommercial License, which permits use, distribution and reproduction in any medium, provided the original work is properly cited and is not used for commercial purposes.

© 2020 The Authors. *Cancer Science* published by John Wiley & Sons Australia, Ltd on behalf of Japanese Cancer Association

1 | INTRODUCTION

Lymph node (LN) metastasis is one of the most important factors associated with cancer mortality and the role of metastatic LNs in systemic metastasis has been recognized for many years.^{1,2} We previously reported that tumor cells that metastasize to an LN can invade blood vessels within the LN and initiate systemic metastasis before the downstream LNs are colonized.^{3,4} This means that a metastatic LN can act as the source of systemic metastasis, which usually indicates a very poor prognosis for the patient.⁵⁻⁷ Thus, tumor progression in LNs must be suppressed in order to prevent systemic metastasis. Systemic chemotherapy, radiotherapy and lymphadenectomy are used as the main treatment strategies for LN metastasis depending on the nodal status. However, these methods have limitations such as invasiveness, lack of selectivity and (for chemotherapy) limited access to LNs. Previously, we have shown that the enhanced permeability and retention (EPR) effect, which underlies the targeting of tumors by systemic chemotherapy, is not expected to occur during early-stage LN metastasis.⁸

Anatomical barriers between the blood circulation and lymphatic network are major obstacles to the effective treatment of LN metastasis. Antitumor agents administered through blood vessels often have poor penetration into intralymphatic tumor lesions, because these relatively small molecules are likely to be reabsorbed by peripheral blood vessels before they are taken up by lymphatic vessels.⁹ We have generated a model of LN metastasis in MXH10/Mo-*lpr/lpr* (MXH10/Mo/*lpr*) mice and used it to develop a novel LDDS that can target tumor cells in LNs during early-stage LN metastasis.^{10,11} Treatment with an anticancer agent and LDDS resulted in notable antitumor effects during the early stage of LN metastasis, was vastly superior to systemic drug delivery, and was without significant adverse effects.^{12,13} An important advantage of the LDDS is that the drug solution can flow directly into downstream LNs to prevent LN metastasis.¹⁴ In the present study, direct injection of drugs under the guidance of high-frequency ultrasound (HF-US) imaging permitted administration of drugs within the target LN and delivery of the drugs to intranodal tumor cells, which contributed to a high response rate for the cis-dichlorodiammineplatinum(II) (CDDP) without any adverse events.^{15,16} Therefore, we defined a series of precise injection of drugs into the target LN as LDDS. The LDDS has the potential to minimize the extent of lymphadenectomy and improve the quality of life of patients with metastatic cancer. However, it remains to be established how best to evaluate the treatment effects using the LDDS.

It has been reported that intranodal pressure (INP, the internal pressure of an LN) is elevated in metastatic LNs in patients with cancer.¹⁷ Previously, we reported that a metastatic LN shows a rise in INP before any change in volume and that INP could be used as a parameter to diagnose early-stage LN metastasis before any detectable increase in LN size had occurred.¹⁸ Solid tumors have high interstitial fluid pressures (IFPs) regardless of the tumor type due to leakage of fluid from abnormal tumor blood vessels and poor drainage of tumor lymph vessels. Previous studies have reported that tumor

IFP was decreased by treatment with hyperthermia¹⁹ or chemotherapy.²⁰ These treatment-associated decreases in IFP are caused by improved blood perfusion, hypoxia, a reduction in tumor collagen content, and an increased number of tumor fibroblasts.²¹ Therefore, tumor IFP is affected not only by cancer cell proliferation but also by destruction of cancer cells in response to therapy. Analogously, if INP were to be associated with tumor cell activity in metastatic LNs, measurement of the changes in the INP of metastatic LNs could potentially be used to monitor the effects of chemotherapeutic agents delivered with an LDDS.

The aim of the present study was to investigate whether INP might be a useful parameter for monitoring the effects of a treatment delivered with LDDS. Therefore, we evaluated whether the administration of CDDP with a LDDS could prevent a progressive increase in INP or even reduce the INP in a metastatic LN. The study used a mouse model of LN metastasis generated by inoculating murine tumor cells into the subiliac LN (SiLN) of MXH10/Mo/*lpr* mice, and the treatment intervention was carried out using a novel LDDS.

2 | MATERIALS AND METHODS

2.1 | Mice

Animal experiments were carried out in accordance with ethical guidelines and approved by the Institutional Animal Care and Use Committee of Tohoku University. For the animal experiments, mice were anesthetized with 2% isoflurane (Abbott Japan) using an inhalation gas anesthesia system for small laboratory animals in order to minimize distress or pain.

MXH10/Mo-*lpr/lpr* (MXH10/Mo/*lpr*) mice (12-17 weeks of age), a congenic strain of MRL/Mp-*lpr/lpr* and C3H/HeJ-*lpr/lpr* mice, were bred under specific pathogen-free conditions in the Animal Research Institute, Graduate School of Medicine, Tohoku University, Sendai, Japan. The anatomical locations and nomenclatures of murine LNs have often been ignored or assigned incorrectly; in the present study we used the term "subiliac LN" instead of "inguinal LN."

2.2 | Cell culture

KM-Luc/GFP cells (mouse malignant fibrous histiocytoma-like [MRL/N-1] cells derived from an MRL/Mp-*gld/gld* mouse expressing a fusion of the luciferase and EGFP genes) were cultured as previously described.¹² FM3A-Luc cells (C3H/He mouse mammary carcinoma cells expressing the luciferase gene) were cultured as previously described.¹⁶

2.3 | Tumor inoculation into the SiLN

A total of 3.3×10^6 cells/mL of KM-Luc/GFP and 5.0×10^7 cells/mL of FM3A-Luc were suspended in 60 μ L PBS (Sigma-Aldrich; 20 μ L) with

400 mg/mL Matrigel (Collaborative Biomedical Products; 40 μ L). Thus, 6.6×10^4 of KM-Luc/GFP cells and 3.0×10^5 of FM3A-Luc cells were inoculated into the SiLN. Accurate inoculation of tumor cells into the SiLN was carried out under the guidance of an HF-US imaging system (Fujifilm VisualSonics) with a mechanical single-element transducer (RMV-710B; central frequency, 25 MHz; axial resolution, 70 mm; lateral resolution, 140 mm; focal length, 15 mm; depth of field, 2.7 mm, Fujifilm VisualSonics). The transducer was fixed to a 3-D stage control system (Mark-204-MS; Sigma Koki). To maintain ultrasound transmission, ultrasound gel was placed on the SiLN. To obtain B-mode images, the RMV-710B transducer was placed on the SiLN, and 60 μ L cell suspension was injected into the SiLN. The B-mode images were acquired from an 18 mm \times 18 mm area.

The inoculation day was defined as day 0. Tumor development in the SiLN was detected and monitored using an in vivo bioluminescence imaging system (IVIS; PerkinElmer) at 1, 3, and 6 days postinoculation of KM-Luc/GFP cells and at 3, 5, 7, and 14 days postinoculation of FM3A-Luc cells.

2.4 | Intranodal delivery of CDDP

Cis-dichlorodiammineplatinum(II) (Wako Pure Chemical Industries) was diluted with saline (Otsuka Pharmaceutical) to a concentration of 2.0 mg/kg. Then 60 μ L CDDP solution was injected into the SiLN on days 1 and 4 in the KM-Luc/GFP group and on day 3 in the FM3A-Luc group, under the guidance of an HF-US imaging system with a 25 MHz transducer (RMV-710B; Fujifilm VisualSonics).

2.5 | Analysis of temporal changes in LN volume

On days 1, 3, and 6 in the KM-Luc/GFP group and days 3, 7, and 14 in the FM3A-Luc group, the SiLN was imaged using an HF-US imaging system with a 25 MHz transducer, and SiLN volume was calculated using VEVO 770 software as described in our previous studies.^{12,13,22}

2.6 | Measurement of intranodal blood vessel density by HF-US imaging

After the measurement of LN volume, 100 μ L microbubbles (Sonazoid; Daiichi Sankyo) was injected through the tail vein to detect the intranodal blood vessels. One minute after injection, 200 images at the maximal cross-sectional area were acquired using HF-US in M-mode and VEVO 770 software. The data were analyzed according to our newly developed method,²³ and an image of the intranodal blood vessels was constructed. Blood vessel density was defined as the ratio of the blood vessel area to the LN area expressed as a percentage. After the intranodal blood vessel density measurements had been made, the INP of the SiLN was recorded using the method described in our previous study.¹⁸ A schematic diagram of the experimental procedure is shown in Figure S1A. The INP was

measured using a 31-G side-hole needle (Lot No. 15113; Ito) (Figure S1B). Data were recorded for 5 minutes.

2.7 | Distribution of INP in SiLN

The distribution of INP was investigated in SiLNs inoculated with KM-Luc/GFP cells ($n = 5$, day 6) or PBS ($n = 5$). The INP was measured using a 31-G side-hole needle (Figure S1B), which was advanced through the SiLN in short steps. The measurement points were defined by dividing the long axis of the SiLN into six parts (Figure S1C). The starting point for the measurement was defined as the location of the needle when its side-hole had just fully entered the SiLN, and the end-point was defined as the location of the needle when it reached the other edge of the SiLN. Data were recorded for 30 seconds at each measurement point.

2.8 | Histological analysis

Tumor-bearing SiLNs were dissected on the final day of each experiment. Harvested samples were fixed in 10% formalin at 4°C for 2-3 days, dehydrated in alcohol, embedded in paraffin, and serially sectioned (2.5-3.0 μ m). Hematoxylin-eosin staining was carried out according to standard procedures. Immunostaining was undertaken to detect blood vessels or lymphatic endothelia as previously described.^{12,13} Briefly, immunostaining of CD31-positive vascular endothelial cells or LYVE-1-positive lymphatic endothelial cells was carried out using a prediluted rabbit anti-CD31 polyclonal Ab (1/100 dilution; sc-1506-R, Santa Cruz Biotechnology) or a rabbit anti-mouse LYVE-1 polyclonal Ab (4 μ g/mL; 103-PA50AG, Cosmo Bio) for 2 hours at room temperature in combination with an anti-rabbit IgG Histofine MAX-PO kit for 16 minutes at room temperature and diaminobenzidine.

2.9 | Statistical analysis

Data are expressed as the mean \pm SD or SEM and were analyzed by one-way ANOVA followed by the post-hoc Tukey-Kramer test. Graphs were constructed using GraphPad Prism 7 (GraphPad Software). The Pearson correlation coefficient was used to investigate any correlations between parameters, and graphs were plotted using Excel (Microsoft).

3 | RESULTS

3.1 | Characteristics of tumor invasion in SiLN

First, we investigated the process of cancer cell inoculation into the SiLN and the subsequent spread of tumor cells within the LN, as these factors are relevant to changes in INP. The needle was

inserted manually into the center of the SiLN (Figure S2A), and 60 μ L tumor cell-containing solution was inoculated into the LN (Figure S2B). The tumor cell-containing solution spread spherically within the SiLN (dotted circle). Figure S2C,D illustrates tumor development for the two different cancer cell types. KM-Luc/GFP cells proliferated in the peripheral area of the LN (Figure S2C), whereas FM3A-Luc cells showed diffuse invasion (Figure S2D). These differences likely arise because the two tumor cell types have differing invasive abilities. KM-Luc/GFP cells have low invasive growth characteristics and form tumor regions with well-defined borders in or near the marginal sinuses. In contrast, FM3A cells have high invasive growth characteristics, proliferate along the trabecular sinus, and invade the cortex and paracortex.^{13,24}

Neither type of tumor cell showed extranodal invasion during the experimental period.

3.2 | Intranodal pressure is uniformly distributed across the long axis of SiLN

To evaluate whether the inoculation procedure affected the distribution of INP within the SiLN, INP was measured at six different points along the long axis of the LN, and any variations in INP were compared between tumor-bearing SiLNs and control SiLNs without tumor (Figure S1A-C). Figure S1D shows the distribution of INP along the long axis of KM-Luc/GFP cell-bearing SiLNs on

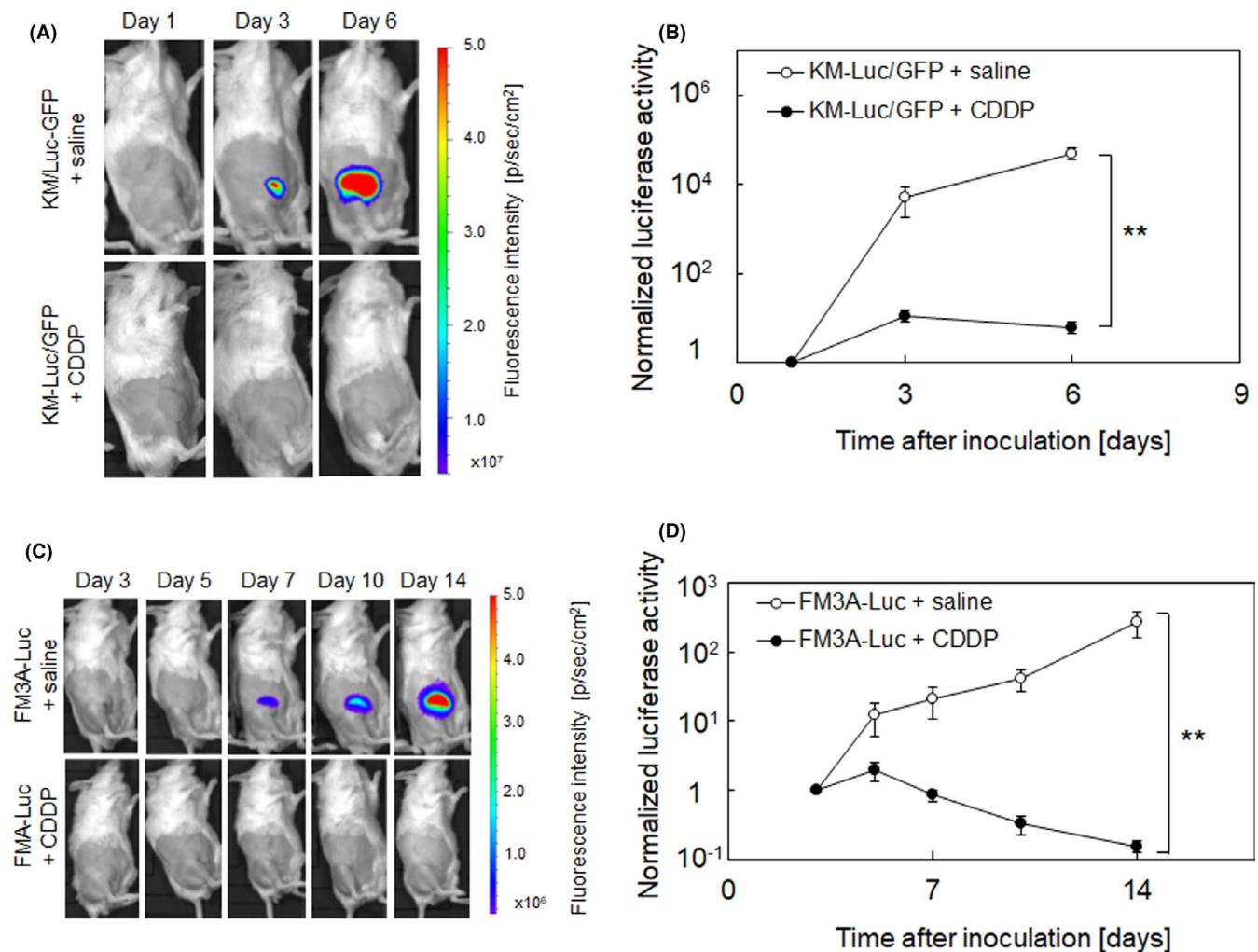


FIGURE 1 Evaluation of the effects of intranodal cis-dichlorodiammineplatinum(II) (CDDP) delivery into a tumor-bearing lymph node (LN) by in vivo bioluminescence imaging. CDDP (2.0 mg/kg in saline) was delivered into the tumor-bearing subiliac LN (SiLN) on days 1 and 4 (KM-Luc/GFP; A, B) or day 3 (FM3A-Luc; C, D). Tumor proliferation was evaluated from measurements of luciferase activity, which was normalized to the value on day 1 (KM-Luc/GFP) or day 3 (FM3A-Luc). A, In vivo bioluminescence imaging of SiLN inoculated with KM-Luc/GFP cells. A solution of CDDP (n = 13) or saline (control, n = 14) was injected into the tumor-bearing SiLN on days 1 and 4 after tumor inoculation. B, Luciferase activity rapidly increased in the control group, but this elevation was suppressed by treatment with CDDP. C, In vivo bioluminescence imaging of SiLN inoculated with FM3A-Luc cells. A solution of CDDP (n = 11) or saline (control, n = 12) was injected into the tumor-bearing SiLN on day 3 after tumor inoculation. D, Although luciferase activity exhibited a progressive increase in the control group (FM3A-Luc + saline), it exhibited a continuous decrease between day 5 and day 14 in the group treated with only a single dose of CDDP (FM3A-Luc + CDDP). Error bars represent SEM. **P < .01

day 6 postinoculation ($n = 5$) and the control SiLNs ($n = 5$). There were no significant differences in INP between the six measurement points in each group (control SiLN group, $P = .995$; tumor-bearing SiLN group, $P = .927$; one-way ANOVA). Thus, INP was distributed uniformly across the SiLN in both control and tumor-bearing LNs.

3.3 | Cis-dichlorodiammineplatinum(II) treatment with LDDS inhibited tumor activity in SiLN

Next, we assessed the treatment effects of CDDP delivered directly into the tumor-bearing SiLN with the LDDS. Figure 1A shows the results of in vivo bioluminescence imaging of the SiLN to detect inoculated KM-Luc/GFP cells. Luciferase activity increased rapidly over time in the control group (KM-Luc/GFP + saline), indicating a substantial proliferation of KM-Luc/GFP cells, whereas treatment with CDDP (KM-Luc/GFP + CDDP) greatly suppressed the elevation in luciferase activity ($P < .01$ at day 6; Figure 1B). Figure 1C shows in vivo bioluminescence

images of the SiLN after the inoculation of FM3A-Luc cells. Although luciferase activity showed a progressive increase in the control group (FM3A-Luc + saline), there was a continuous decrease between day 5 and day 14 ($P < .01$ on day 14) in the group treated with only a single dose of CDDP (FM3A-Luc + CDDP; Figure 1D).

3.4 | Cis-dichlorodiammineplatinum(II) treatment with LDDS reduced volume of tumor-bearing SiLN and inhibited increase in intranodal blood vessel density in MXH10/Mo/lpr mice

Subsequently, we investigated how CDDP treatment with a LDDS affected the morphology of the tumor-bearing SiLN. Figure 2 shows representative HF-US images of the SiLN (dashed line indicates the border of the SiLN) and measurements of SiLN volume and blood vessel density before and after delivery of CDDP or saline (control). In Figure 2A, the panel labeled "CDDP" shows a tumor-free SiLN (ie no inoculation with cancer cells) after CDDP treatment. Treatment

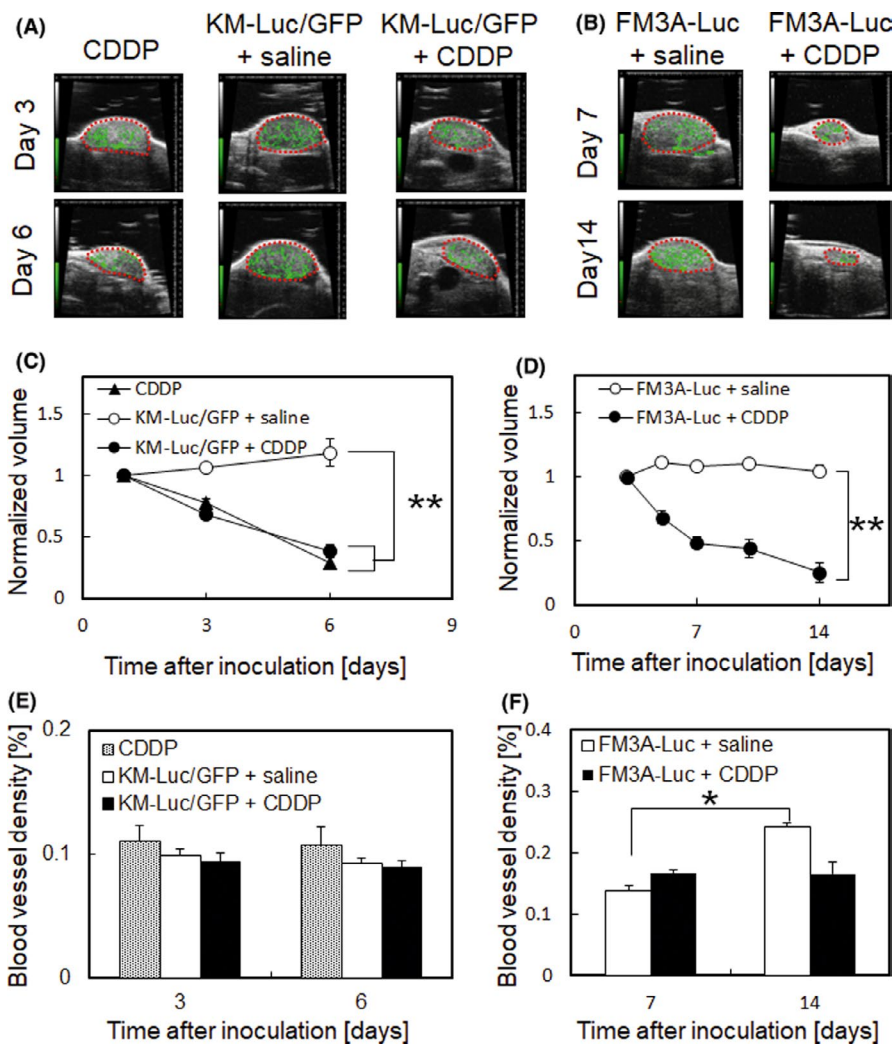


FIGURE 2 Temporal changes in the volume and intranodal blood vessel density of the tumor-bearing subiliac lymph node (SiLN) with or without cis-dichlorodiammineplatinum(II) (CDDP) treatment. The LN volume was measured on days 1, 3, and 6 (KM-Luc/GFP; A, C) or days 3, 5, 7, 10, and 14 (FM3A-Luc; B, D) using a contrast-enhanced high-frequency ultrasound imaging system. Dashed lines indicate SiLN borders. CDDP given with the lymphatic drug delivery system (LDDS) reduced the volume of SiLNs inoculated with KM-Luc/GFP or FM3A-Luc cells. Reconstruction of the intranodal blood vessels (green region) and calculation of blood vessel density were carried out using a high-accuracy ultrasound contrast agent detection method on days 3 and 6 (KM-Luc/GFP; E) or days 7 and 14 (FM3A-Luc; F). The numbers of mice used in the study were: CDDP ($n = 5$), KM-Luc/GFP + saline ($n = 14$), KM-Luc/GFP + CDDP ($n = 13$), FM3A-Luc + saline ($n = 12$), and FM3A-Luc + CDDP ($n = 11$). Error bars indicate SEM. * $P < .05$, ** $P < .01$

with CDDP reduced the volumes of SiLNs inoculated with KM-Luc/GFP cells (Figure 2A,C) or FM3A-Luc cells (Figure 2B,D). High frequency-US with an ultrasound contrast agent was used to reconstruct an image of the intranodal blood vessels (green region) and calculate blood vessel density on days 3 and 6 (KM-Luc/GFP cells) or days 7 and 14 (FM3A-Luc cells). In mice inoculated with KM-Luc/GFP cells, there was no change in the intranodal blood vessel density of the tumor-bearing SiLN between days 3 and 6, and CDDP had no effect on blood vessel density (Figure 2E). However, in mice inoculated with FM3A-Luc cells, there was an increase in the blood vessel density of the tumor-bearing SiLN between days 7 and 14 (Figure 2F, $P < .05$), and direct intranodal injection of CDDP suppressed this increase in blood vessel density.

3.5 | Intranodal pressure had no correlation with changes in volume of tumor-bearing SiLN

In order to establish whether INP might be influenced by changes in the volume of a metastatic LN, the correlation between INP and change in tumor-bearing SiLN volume was compared with that between IFP and solid tumor volume. Figure 3A,B show the relation between tumor volume (horizontal axis) and IFP (vertical axis) for solid tumors comprised of KM-Luc/GFP cells and FM3A-Luc cells, respectively. There was a strong positive correlation between tumor volume and IFP for both types of solid tumor (KM-Luc/GFP cells: $R^2 = 0.866$, $P < .0001$; FM3A-Luc cells: $R^2 = 0.894$, $P = .0001$). The correlations between change in tumor-bearing SiLN volume and INP are shown in Figure 3C (KM-Luc/GFP cells) and Figure 3D (FM3A-Luc cells); the LN volume change was calculated as the LN volume on day 6 (KM-Luc/GFP cells) or day 14 (FM3A-Luc cells) minus the LN volume on day 0 (the day of tumor cell inoculation). There were no significant correlations between changes in tumor-bearing SiLN volume and INP for either type of inoculated cancer cell (KM-Luc/GFP

cells: $R^2 = 0.021$, $P = .760$; FM3A-Luc cells: $R^2 = 0.008$, $P = .850$). These results indicated that INP is not correlated with a change in tumor-bearing SiLN volume.

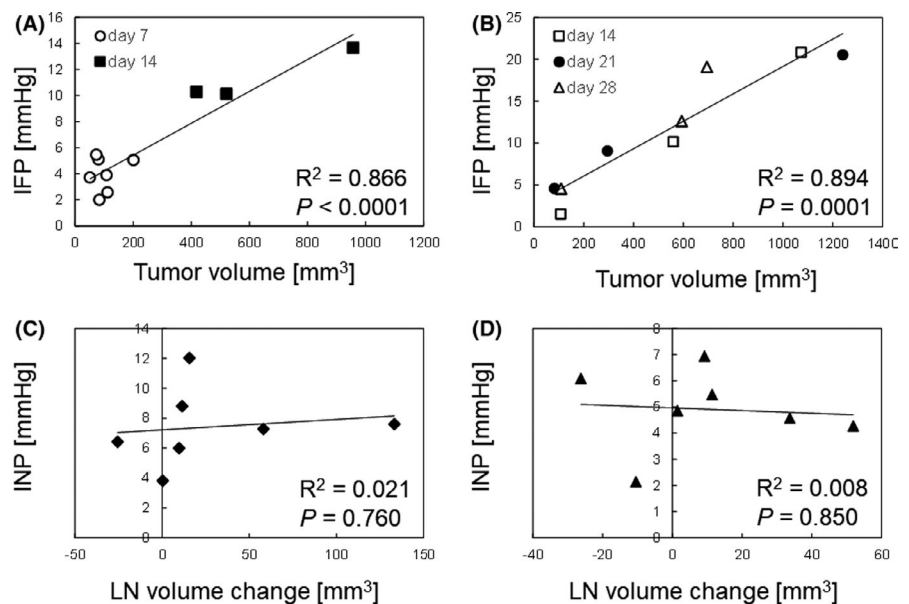
3.6 | Intranodal pressure changes reflect antitumor effects of CDDP treatment using LDDS

Next we investigated whether the anticancer actions of CDDP might be associated with changes in INP. Figure 4A shows the temporal changes in INP for SiLNs inoculated with KM-Luc/GFP cells. Control SiLNs (injected with saline instead of KM-Luc/GFP cells) treated with CDDP (PBS + CDDP) showed little change in INP over time. By contrast, SiLNs inoculated with KM-Luc/GFP cells and not treated with CDDP (KM-Luc/GFP + saline) showed a progressive increase in INP between days 3 and 6 (day 3, $n = 8$; day 6, $n = 7$). However, CDDP treatment to SiLNs inoculated with KM-Luc/GFP cells (KM-Luc/GFP + CDDP) resulted in a significant reduction in INP on day 6 ($P < .01$ vs KM-Luc/GFP + saline). The temporal changes in INP for SiLNs inoculated with FM3A-Luc cells are shown in Figure 4B. For tumor-bearing SiLNs not treated with CDDP (FM3A-Luc + saline), INP showed a substantial elevation on days 7 and 14 and was higher on day 7 than on day 14. Notably, CDDP treatment with the LDDS (FM3A-Luc + CDDP) resulted in a significant reduction in INP on day 7 ($P < .05$ vs FM3A-Luc + saline) and day 14 ($P < .01$ vs FM3A-Luc + saline).

3.7 | Histological evaluation of SiLN after CDDP treatment with LDDS

Finally, histopathological analyses of tumor-bearing SiLNs on day 6 (KM-Luc/GFP cells) or day 14 (FM3A-Luc cells) were carried out to evaluate the antitumor effects of CDDP applied using the LDDS. Figure 5 shows representative microscopic images of the

FIGURE 3 Intranodal pressure (INP) had no correlation with changes in tumor-bearing lymph node (LN) volume. Correlation between tumor volume (mm^3) and interstitial fluid pressure (IFP) (mm Hg) for intradermal solid tumors composed of KM-Luc/GFP cells (A) or FM3A-Luc cells (B). \circ , day 7 ($n = 7$); \blacksquare , day 14 ($n = 3$); \square , day 14 ($n = 3$); \bullet , day 21 ($n = 3$); \triangle , day 28 ($n = 3$) posttumor inoculation. Correlation between LN volume change (mm^3) and INP (mm Hg) for subiliac LNs inoculated with KM-Luc/GFP cells (C) or FM3A-Luc cells (D). LN volume change was calculated as the LN volume on day 6 (KM-Luc/GFP) or day 14 (FM3A-Luc) after tumor cell inoculation minus the LN volume on day 0



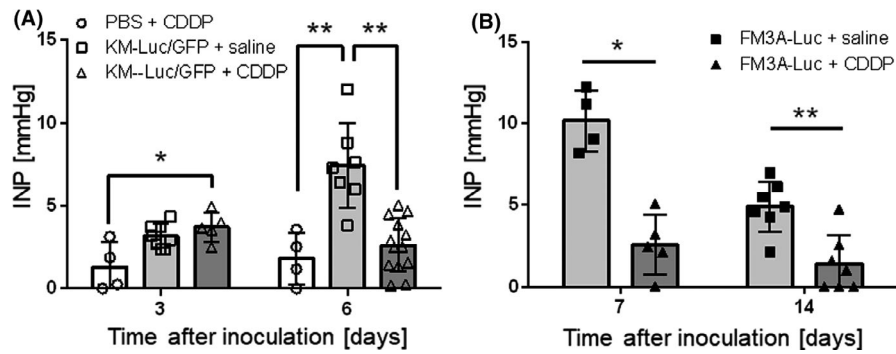


FIGURE 4 Intranodal pressure (INP) reflects the antitumor effects of cis-dichlorodiammineplatinum(II) (CDDP) given with a lymphatic drug delivery system. A, Temporal changes in INP for subiliac lymph nodes (SiLN) inoculated with KM-Luc/GFP cells. The INP of the non-cancerous SiLN was approximately 0 mm Hg on day 0. INP increased progressively in SiLN inoculated with KM-Luc/GFP cells and injected with saline as a control for CDDP (day 3, $n = 8$; day 6, $n = 7$). However, CDDP treatment (KM-Luc/GFP + CDDP) slightly reduced the INP between day 3 ($n = 5$) and day 6 ($n = 13$), and the value on day 6 was significantly lower than that of the KM-Luc/GFP + saline group on day 6. B, Temporal changes in INP for SiLN inoculated with FM3A-Luc cells. The INP of the control group (FM3A-Luc + saline) showed a substantial elevation on day 7 ($n = 4$) followed by a decrease on day 14 ($n = 7$). Treatment with CDDP (FM3A-Luc + CDDP) resulted in significant decreases in INP on day 7 ($n = 5$) and day 14 ($n = 8$). Error bars indicate SD. * $P < .05$, ** $P < .01$

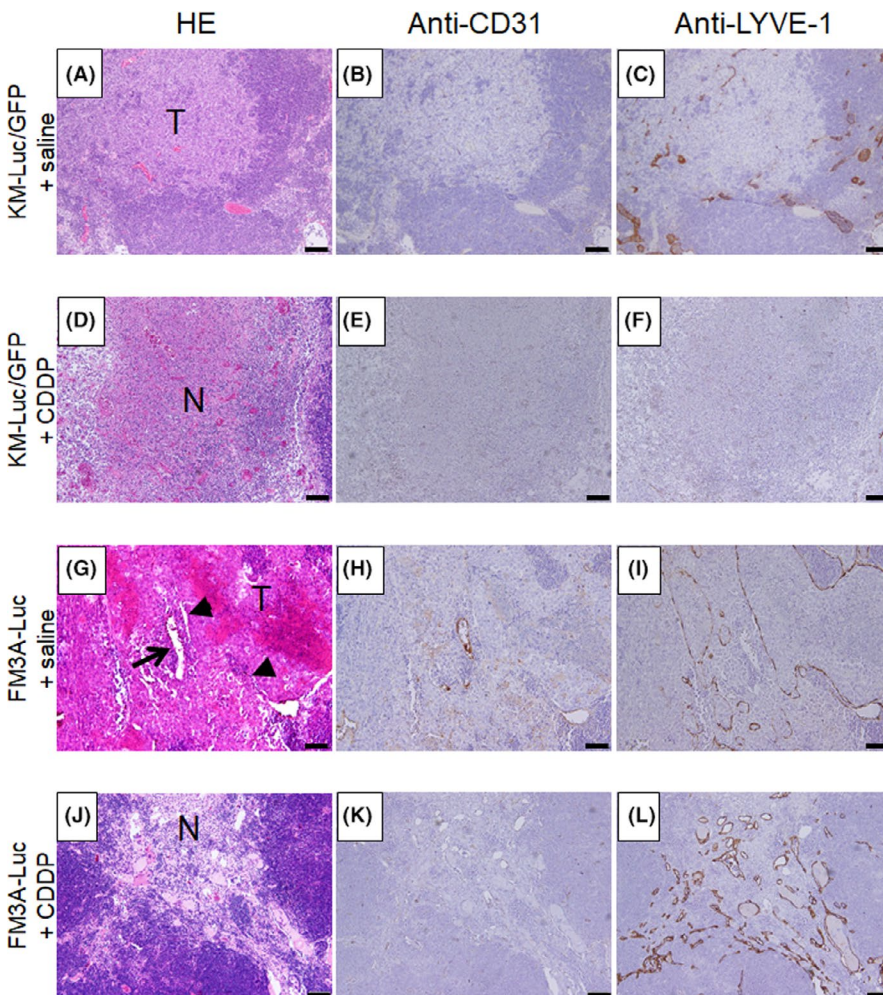


FIGURE 5 Histological analysis of mouse tumor-bearing subiliac lymph node (SiLN) on day 6 (KM-Luc/GFP) or day 14 (FM3A-Luc) after cis-dichlorodiammineplatinum(II) (CDDP) treatment with the lymphatic drug delivery system. H&E staining (A, D, G, J), anti-CD31 immunostaining (B, E, H, K), and anti-LYVE-1 immunostaining (C, F, I, L) were carried out to identify the tumor lesion, vascular endothelium, and lymphatic endothelium of the SiLN, respectively. For both tumor cell lines, SiLN treated with CDDP showed sporadic necrotic foci within the tumor region (D, J). In addition, areas of cell loss were observed within the tumor region in the FM3A-Luc + CDDP group (J). In contrast, proliferating tumor cells were detected in the FM3A-Luc + saline group, and necrotic foci and regions of cell loss were not observed (G). Expanded CD31-positive blood vessels and LYVE-1-positive lymph vessels were observed in the FM3A-Luc + CDDP group (K, L) but not in the other groups (B, C, E, F, H, I). Arrow and arrowheads represent blood vessels and lymph vessels, respectively (G). Scale bar = 50 μm . N, necrosis; T, tumor

tumor-bearing SiLN stained with H&E (Figure 5A,D,G,J) or immunostained for CD31 (Figure 5B,E,H,K) or LYVE-1 (Figure 5C,F,I,L). In the groups given CDDP using the LDDS, sporadic necrotic foci were

detected within the tumor region (Figure 5D,J). In contrast, proliferating tumor cells rather than necrotic foci or regions of cell loss were observed in the groups not treated with CDDP (Figure 5A,G).

4 | DISCUSSION

We report that the direct delivery of an anticancer drug into the lymphatic system using a novel LDDS was an effective treatment for early-stage LN metastasis in a mouse model and that INP reflects tumor activity in the tumor-bearing LN. Therefore, measurement of INP could be a useful method to evaluate the therapeutic effects of cancer treatment delivered using a LDDS.

A notable finding of the present study was that proliferation of intranodal tumor cells (Figure 1) was associated with an increase in INP but no change in the volume of the tumor-bearing SiLN (Figures 2C,D and 4). In a clinical study of patients with breast cancer, Nathanson et al¹⁷ reported no correlation between LN metastasis and LN size but found a clear association between LN metastasis and INP elevation. During the avascular proliferation phase of a primary solid tumor, tumor blood vessels are formed from the existing vasculature and supply oxygen and nutrients that facilitate tumor proliferation.²¹ The tumor blood vessels are abnormal in structure and contain open spaces as large as 2 μm between the vascular endothelial cells, which contribute to vascular hyperpermeability and fluid leakage. This transvascular "ooze" could induce an IFP elevation in a primary solid tumor^{25,26} and obstruct drug penetration deep into tumor lesions.²⁷ However, we and others have recently found that angiogenesis and the EPR effect do not occur during the early phase of LN metastasis, even at the tumor expansion stage.^{8,28} As draining LNs already contain an abundance of blood vessels before the arrival of any tumor cells,²⁹ the formation of additional blood vessels to supply oxygen or nutrients to metastatic tumor cells is not required, and thus vascular hyperpermeability might not be induced under these conditions. If so, the increase in INP reported in our study would not be due to fluid leakage from tumor-induced blood vessels.

An accumulation of *Ipr* T cells ($\text{CD4}^-\text{CD8}^-\text{B220}^+$) was associated with adenopathy of *MXH/Mo/Ipr* mice. Treatment with CDDP could kill many of the *Ipr* T cells that caused the reduction in the volume of the LN. In addition, CDDP might damage the bone marrow that supplies immune cells and thereafter the volume of the LNs given in CDDP treatment did not recover easily.³⁰

In the intradermal solid tumor (Figure S3), the tumor can have unlimited growth as long as the oxygen and nutrients are supplied from the existing blood vessels or newly formed tumor blood vessels. However, tumor cells in LN could grow in the lymphatic sinuses where the blood vessels are scarce. As we discussed in our previous work,^{8,18} tumor angiogenesis in the metastatic LN was not induced in the early phase of LN metastasis. If the tumor cells encounter blood vessels in the LN, the blood vessels play a role as a metastatic pathway, not the nutrient vessels. In addition, lymphocytes and other immune cells are densely packed in the LN, which could limit the space where tumor cells could grow. This is why the scale of LN volume change rate (Figure 3C,D) was smaller than the increase in the solid tumor volume (Figure 3A,B).

Regrettably, it is difficult to measure the volume of the intranodal tumor mass. However, there was a positive correlation between

the volume of solid tumor and luciferase activity (Figure S3A,B, KM-Luc/GFP; Figure S3C,D, FM3A-Luc). Thus, we can predict the intranodal tumor volume based on the luciferase activity of the SiLN.

Generally, the LN has little interstitial space and is densely packed with cells, which suggests that the LN has an incompressible material property, regardless of the presence or location of a tumor. The INP is assumed to be uniformly distributed throughout the SiLN^{27,31}; that is, tumor cell proliferation within the capsular structure of LN at the early stage of LN metastasis did not contribute to the increase in LN volume, but the properties of increasing tumor volume might be transformed into energy for a pressure increase during an isovolumic change. Therefore, the stress against the surrounding lymphoid tissues during intranodal tumor proliferation might not be attenuated in the interstitial area and delivered to the entire LN.

Debate remains as to how metastatic cells are disseminated to distant organs through mechanisms involving the lymphatic network. In our previous study, we revealed that intranodal lymphatic networks could connect to the systemic circulation of the LN, depending on the intranodal mechanical pressure.⁴ Interestingly, lymphatic flow in a tumor-bearing LN with a high INP was preferentially directed to the venous vasculature rather than the downstream lymphatic network in the metastatic mouse model. Clinically, LN metastasis is usually diagnosed based on changes in LN size, shape, and blood flow,³² but at this stage tumor cells might already have had the chance to disseminate to distant organs. Rofstad et al³³ pointed out that IFP in a primary tumor was positively correlated with the incidence of LN metastasis and pulmonary metastasis. Here, we have described a novel diagnostic method of determining intranodal tumor status based on INP measurement. Needles for measurement of INP can easily access LNs located under or near the skin. A raised INP in our mouse model of a metastatic LN is associated with an increased risk of LN-mediated hematogenous metastasis. However, treatment with an anticancer agent with an LDDS can reduce INP and decrease the risk of systemic metastasis. However, we have to pay attention to the fact that the relationship between LN metastasis and distant metastasis in humans remain to be elucidated. Some studies have insisted that a weak relationship exists between LN metastasis and distant metastasis, based on phylogenetic analysis.³⁴⁻³⁶ In some cases, metastatic cells in regional LN and distant organs originated from common lesions, indicating that some cases of LN metastasis in humans might contribute to distant metastasis.³⁷

In conclusion, we have shown that the elevation of INP in a metastatic LN can be reduced by CDDP treatment with an LDDS and that INP alterations reflect the therapeutic effects of the drug. We suggest that the mechanism of INP elevation in metastatic LNs is different from that of IFP elevation in solid tumors, which is mainly induced by mechanical forces due to tumor proliferation rather than fluid leakage resulting from tumor angiogenesis. Little correlation was found between INP and changes in metastatic LN volume. Importantly, CDDP delivery with a LDDS caused shrinkage of the intranodal tumor mass and a lowering of INP, which has the potential to prevent hematogenous metastasis in our mouse model. As such, INP could be an important parameter for evaluating the treatment

effects of intralymphatic chemotherapy and in deciding subsequent treatment strategies for patients with cancer.

ACKNOWLEDGMENTS

The authors would like to thank T. Sato for technical assistance and the Biomedical Research Core of Tohoku University Graduate School of Medicine for technical support. The study was supported by Japan Society for the Promotion of Science KAKENHI grant numbers 17K13039 (SK), 19K16622 (SK), 19K22692 (KS), 17K20077 (TK), 17H00865 (TK), 19K22941 (TK), and 20H00655 (TK).

CONFLICT OF INTEREST

The authors declare that they have no competing interests.

ORCID

Tetsuya Kodama  <https://orcid.org/0000-0003-4727-9558>

REFERENCES

- Fisher B, Fisher ER. Transmigration of lymph nodes by tumor cells. *Science*. 1966;152:1397-1398.
- Karaman S, Detmar M. Mechanisms of lymphatic metastasis. *J Clin Invest*. 2014;124:922-928.
- Shao L, Ouchi T, Sakamoto M, Mori S, Kodama T. Activation of latent metastases in the lung after resection of a metastatic lymph node in a lymph node metastasis mouse model. *Biochem Biophys Res Commun*. 2015;460:543-548.
- Takeda K, Mori S, Kodama T. Study of fluid dynamics reveals direct communications between lymphatic vessels and venous blood vessels at lymph nodes of mice. *J Immunol Methods*. 2017;445:1-9.
- Brown M, Assen FP, Leithner A, et al. Lymph node blood vessels provide exit routes for metastatic tumor cell dissemination in mice. *Science*. 2018;359:1408-1411.
- Kodama T, Mori S, Nose M. Tumor cell invasion from the marginal sinus into extranodal veins during early-stage lymph node metastasis can be a starting point for hematogenous metastasis. *J Cancer Metastasis Treat*. 2018;4:56.
- Pereira ER, Kedrin D, Seano G, et al. Lymph node metastases can invade local blood vessels, exit the node, and colonize distant organs in mice. *Science*. 2018;359:1403-1407.
- Mikada M, Sukhbaatar A, Miura Y, et al. Evaluation of the enhanced permeability and retention effect in the early stages of lymph node metastasis. *Cancer Sci*. 2017;108:846-852.
- Swartz MA. The physiology of the lymphatic system. *Adv Drug Deliv Rev*. 2001;50:3-20.
- Shao L, Mori S, Yagishita Y, et al. Lymphatic mapping of mice with systemic lymphoproliferative disorder: usefulness as an inter-lymph node metastasis model of cancer. *J Immunol Methods*. 2013;389:69-78.
- Shao L, Takeda K, Kato S, Mori S, Kodama T. Communication between lymphatic and venous systems in mice. *J Immunol Methods*. 2015;424:100-105.
- Kato S, Mori S, Kodama T. A Novel treatment method for lymph node metastasis using a lymphatic drug delivery system with nano/microbubbles and ultrasound. *J Cancer*. 2015;6:1282-1294.
- Kato S, Shirai Y, Sakamoto M, Mori S, Kodama T. Use of a lymphatic drug delivery system and sonoporation to target malignant metastatic breast cancer cells proliferating in the marginal sinuses. *Sci Rep*. 2019;9:13242.
- Tada A, Horie S, Mori S, Kodama T. Therapeutic effect of cisplatin given with a lymphatic drug delivery system on false-negative metastatic lymph nodes. *Cancer Sci*. 2017;108:2115-2121.
- Sato T, Mori S, Arai Y, Kodama T. The combination of intralymphatic chemotherapy with ultrasound and nano-/microbubbles is efficient in the treatment of experimental tumors in mouse lymph nodes. *Ultrasound Med Biol*. 2014;40:1237-1249.
- Sato T, Mori S, Sakamoto M, Arai Y, Kodama T. Direct delivery of a cytotoxic anticancer agent into the metastatic lymph node using nano/microbubbles and ultrasound. *PLoS One*. 2015;10:e0123619.
- Nathanson SD, Mahan M. Sentinel lymph node pressure in breast cancer. *Ann Surg Oncol*. 2011;18:3791-3796.
- Miura Y, Mikada M, Ouchi T, et al. Early diagnosis of lymph node metastasis: importance of intranodal pressures. *Cancer Sci*. 2016;107:224-232.
- Leunig M, Goetz AE, Dellian M, et al. Interstitial fluid pressure in solid tumors following hyperthermia: possible correlation with therapeutic response. *Cancer Res*. 1992;52:487-490.
- Fan Y, Du W, He B, et al. The reduction of tumor interstitial fluid pressure by liposomal imatinib and its effect on combination therapy with liposomal doxorubicin. *Biomaterials*. 2013;34:2277-2288.
- Jain RK, Martin JD, Stylianopoulos T. The role of mechanical forces in tumor growth and therapy. *Annu Rev Biomed Eng*. 2014;16:321-346.
- Kato S, Shirai Y, Kanzaki H, Sakamoto M, Mori S, Kodama T. Delivery of molecules to the lymph node via lymphatic vessels using ultrasound and nano/microbubbles. *Ultrasound Med Biol*. 2015;41:1411-1421.
- Ito K, Noro K, Yanagisawa Y, et al. High-accuracy ultrasound contrast agent detection method for diagnostic ultrasound imaging systems. *Ultrasound Med Biol*. 2015;41:3120-3130.
- Fujii H, Horie S, Sukhbaatar A, et al. Treatment of false-negative metastatic lymph nodes by a lymphatic drug delivery system with 5-fluorouracil. *Cancer Med*. 2019;8:2241-2251.
- Hobbs SK, Monsky WL, Yuan F, et al. Regulation of transport pathways in tumor vessels: role of tumor type and microenvironment. *Proc Natl Acad Sci U S A*. 1998;95:4607-4612.
- Raleigh JA, Calkins-Adams DP, Rinker LH, et al. Hypoxia and vascular endothelial growth factor expression in human squamous cell carcinomas using pimonidazole as a hypoxia marker. *Cancer Res*. 1998;58:3765-3768.
- Jain RK, Baxter LT. Mechanisms of heterogeneous distribution of monoclonal antibodies and other macromolecules in tumors: significance of elevated interstitial pressure. *Cancer Res*. 1988;48:7022-7032.
- Jeong HS, Jones D, Liao S, et al. Investigation of the lack of angiogenesis in the formation of lymph node metastases. *J Natl Cancer Inst*. 2015;107.
- Qian CN, Berghuis B, Tsarfaty G, et al. Preparing the "soil": the primary tumor induces vasculature reorganization in the sentinel lymph node before the arrival of metastatic cancer cells. *Cancer Res*. 2006;66:10365-10376.
- Attia SM. The impact of quercetin on cisplatin-induced clastogenesis and apoptosis in murine marrow cells. *Mutagenesis*. 2010;25:281-288.
- Boucher Y, Baxter LT, Jain RK. Interstitial pressure gradients in tissue-isolated and subcutaneous tumors: implications for therapy. *Cancer Res*. 1990;50:4478-4484.
- Wunderbaldinger P. Problems and prospects of modern lymph node imaging. *Eur J Radiol*. 2006;58:325-337.
- Rofstad EK, Tunheim SH, Mathiesen B, et al. Pulmonary and lymph node metastasis is associated with primary tumor interstitial fluid pressure in human melanoma xenografts. *Cancer Res*. 2002;62:661-664.
- Reiter JG, Hung WT, Lee IH, et al. Lymph node metastases develop through a wider evolutionary bottleneck than distant metastases. *Nat Genet*. 2020;52:692-700.
- Ullah I, Karthik GM, Alkodsai A, et al. Evolutionary history of metastatic breast cancer reveals minimal seeding from axillary lymph nodes. *J Clin Invest*. 2018;128:1355-1370.

36. Wei Q, Ye Z, Zhong X, et al. Multiregion whole-exome sequencing of matched primary and metastatic tumors revealed genomic heterogeneity and suggested polyclonal seeding in colorectal cancer metastasis. *Ann Oncol*. 2017;28:2135-2141.
37. Naxerova K, Reiter JG, Brachtel E, et al. Origins of lymphatic and distant metastases in human colorectal cancer. *Science*. 2017;357:55-60.

How to cite this article: Kato S, Takeda K, Sukhbaatar A, et al. Intranodal pressure of a metastatic lymph node reflects the response to lymphatic drug delivery system. *Cancer Sci*. 2020;111:4232-4241. <https://doi.org/10.1111/cas.14640>

SUPPORTING INFORMATION

Additional supporting information may be found online in the Supporting Information section.